MicroRNA-1226-3p has a tumor-promoting role in osteosarcoma

YONG LI[1], DAI SONG[2], TING AN[3], JIE LIU[3], QIAN YANG[3] and SHAOKUI NAN[1]

[1]Department of Orthopedics, Sixth Medical Center of The PLA General Hospital, Beijing 100048;
[2]Community Health Service Center of South Railway Station, Chengdu, Sichuan 610042;
[3]Department of Pediatric Surgery, West China Hospital, Sichuan University, Chengdu, Sichuan 610041, P.R. China

Received October 3, 2020; Accepted March 22, 2021

DOI: 10.3892/ol.2021.12735

Abstract. Osteosarcoma is a malignant bone tumor that commonly occurs in young individuals. It accounts for 10% of solid tumors in those who are 15-19 years old. MicroRNA (miRNA/miR) dysregulation serves a crucial role in the molecular mechanism of osteosarcoma. The present study reported a novel miRNA (miR-1226-3p) and investigated its function in osteosarcoma. miR-1226-3p mimics and miR-1226-3p antisense oligonucleotides were transfected into human osteosarcoma SaOS-2 cells to alter miR-1226-3 expression, while the hFOB 1.19 cell line was used as the control. The apoptosis rate was analyzed using a dead cell apoptosis kit. TNF receptor-associated factor 3 (TRAF3) protein expression was assayed by western blotting. The results of bioinformatics and clinical specimen analyses revealed that higher expression levels of miR-1226-3p were associated with lower survival rates. Additionally, the results of experiments on cultured cells revealed that miR-1226-3p promoted the proliferation of SaOS-2 cells, while miR-1226-3p inhibition decreased cell proliferation and increased apoptosis. Furthermore, it was revealed that miR-1226-3p targeted TRAF3 in SaOS-2 cells. In conclusion, the present study suggested that miR-1226-3p promoted the proliferation of osteosarcoma cells.

Introduction

Osteosarcoma is a malignant tumor derived from bone, and it most commonly occurs in adolescents, accounting for 10% of solid tumors in those who are 15-19 years old (1-3). In 2014, there were ~24,000 newly diagnosed cases of primary bone cancer and 17,200 deaths due to primary bone cancer in China (4). The crude incidence rate of primary bone cancer is 1.76/100,000, and the age-standardized incidence rate by the Chinese standard population is 1.35/100,000 (4).

Correspondence to: Dr Shaokui Nan, Department of Orthopedics, Sixth Medical Center of The PLA General Hospital, 6 Fucheng Road, Haidian, Beijing 100048, P.R. China
E-mail: nghguke@yeah.net

Key words: microRNA-1226-3p, osteosarcoma, cell proliferation, apoptosis

MicroRNAs (miRNAs) are small, highly conserved, non-coding RNA molecules involved in regulating gene expression. They target mRNA molecules for cleavage or translational repression, resulting in the degradation of mRNA and/or the inhibition of mRNA translation (5). Studies have shown that miRNAs may serve important roles in the molecular mechanism of osteosarcoma (6,7).

In the present study, a novel miRNA that may serve a role in the pathogenesis of osteosarcoma was identified. Raw miRNA expression data was downloaded from The Cancer Genome Atlas (TCGA), which is a landmark cancer genomics program that characterizes >20,000 primary cancers of all types. The aim of the TCGA database is to create a comprehensive 'atlas' of cancer genomic profiles by cataloging and discovering major cancer-causing genomic alterations (8). By searching for novel miRNAs associated with the survival of patients with osteosarcoma, miR-1226-3p was identified as a prime candidate. Some studies have revealed that miR-1226-3p functions as a tumor suppressor and may be associated with tamoxifen resistance in breast cancer (9,10). Furthermore, in a recent study, the role of miR-1226-3p in hepatocellular carcinoma was evaluated, revealing that miR-1226-3p expression was downregulated in patients with hepatocellular carcinoma with progressive disease that developed following sorafenib treatment through the inhibition of dual specificity protein phosphatase 4 protein expression (11). However, the role of miR-1226-3p in osteosarcoma remains unknown and was therefore investigated in the present study.

Materials and methods

Patients and tissue samples. A total of 35 pairs of osteosarcoma and matched adjacent normal tissues (~1 cm from tumor) were collected from patients (sex rate female/male, 17/18; age range, 6-60 years; mean age, 14.2 years) at the Department of Pediatric Surgery, West China Hospital, Sichuan University (Chengdu, China). The clinical data of the 35 patients are listed in Table SI. The stage of the 35 patients was based on the TNM staging system (12). The patient recruitment took place between February 2013 and December 2014. The histopathological diagnoses of the 35 paired samples were reviewed by a senior pathologist in the Department of Pathology of West China Hospital. The Ethics Committee of Sichuan University approved the usage of the patients' clinical data and tissue samples, and all patients or their guardians provided written informed consent for the use of their clinical information and tissue samples. The inclusion criteria were as

follows: i) Histological diagnosis of high-grade osteosarcoma, ii) no prior history of lenvatinib treatment, iii) life expectancy of ≥12 weeks, and iv) adequate organ function per blood work results. The exclusion criteria were: i) Any active infection, and ii) history of radiotherapy or chemotherapy.

Bioinformatics analysis. For TCGA analysis, the pan-cancer miRNA expression dataset (pancanMiRs_EBadjOnProtocolPlatform WithoutRepsWithUnCorrect MiRs_08_04_16.xena) and clinical information dataset (Survival_Supplemental Table_S1_20171025_xena_sp) were downloaded using the Xena Browser (https://xenabrowser.net/). The datasets were processed with the dplyr and tribble packages (13). The miRNA expression dataset and clinical information dataset were then merged, and the miRNA information from patients with sarcoma was extracted for survival analysis. The survminer package (https://cran.r-project.org/web/packages/survminer/index.html) was installed in the R language for survival analysis. The clinical data of the patients from TCGA are listed in Table SII. In summary, the total number of patients with osteosarcoma from TCGA was 368 (sex ratio male:female, 160:208; mean age ± SD, 66±14.77 years; age range, 20-90 years). The most common clinicopathological subtypes were myxofibrosarcoma (11%), leiomyosarcoma (42%) and dedifferentiated liposarcoma (20%).

Cell culture. Human osteosarcoma SaOS-2 cells (ATCC HTB-85™) and fetal human osteoblastic hFOB 1.19 cells were purchased from the American Type Culture Collection. SaOS-2 cells were cultured in McCoy's 5A (Modified) medium (cat. no. 16600108; Thermo Fisher Scientific, Inc.) with 10% FBS (cat. no. 16140071; Thermo Fisher Scientific, Inc.). hFOB 1.19 cells were cultured in DMEM (cat. no. 30030; Thermo Fisher Scientific, Inc.) with 2.5 mM L-glutamine, 0.3 mg/ml G418 and 10% FBS. The cells were placed in a cell incubator with 5% CO_2 at 37˚C.

Transfections. miR-1226-3p mimics and miR-1226-3p antisense oligonucleotides (ASOs) were separately transfected into cells in order to increase or decrease miR-1226-3p expression, respectively. The miR-1226-3p mimics, miR-1226-3p ASOs and the respective scrambled negative controls (NCs) were designed and constructed by Sangon Biotech Co., Ltd. The sequences of the miR-1226-3p mimics and miR-1226-3p ASOs were as follows: miR-1226-3p mimics, 5'-UCACCAGCCCUGUGUUCCCUAG-3'; miR-1226-3p ASOs, 5'-AGUGGCGGGACACAAGGGAAAAAA-3'; miR-1226-3p NC mimics, 5'-CGGUACGAUCGCGGCGGGAUAUC-3'; and miR-1226-3p NC ASOs, 5'-GCCAUGCUAGCGCCGCCCUAUAG-3'. Transfections were performed using Lipofectamine® 2000 (cat. no. 11668019; Thermo Fisher Scientific, Inc.) according to the manufacturer's protocol. Briefly, cells were seeded into 24-well plates at a density of $5x10^4$ cells/well. miR-1226-3p mimics or miR-1226-3p ASOs (final concentration, 300 nM) were separately diluted in 50 μl Opti-MEM™ Reduced Serum Medium (Gibco; Thermo Fisher Scientific, Inc.) without serum. Lipofectamine 2000 was mixed gently before use, and 1 μl was diluted in 50 μl Opti-MEM Reduced Serum Medium. After incubation for 5 min, the miRNAs (miR-1226-3p mimics or miR-1226-3p ASOs) were separately combined with the diluted Lipofectamine 2000, then mixed gently and incubated for 20 min at room temperature. Finally, miRNA mimic-Lipofectamine 2000 or miRNA ASO-Lipofectamine 2000 mixtures were added to the wells containing cells and medium. Cells were transfected for 20 min at 37˚C. TRAF3 overexpression was achieved via transfection of the pcDNA3.1-TRAF3 plasmid. The pcDNA3.1-TRAF3 plasmid and NC plasmid (containing a scrambled shNC sequence) was designed and constructed by Sangon Biotech Co., Ltd. Similarly, the plasmids (500 ng) were transfected into cells using Lipofectamine 2000 as aforementioned for 20 min at 37˚C, and then cells were incubated at 37˚C overnight. Subsequent experiments were performed the next day.

Reverse transcription-quantitative (RT-q)PCR. The expression levels of miR-1226-3p in tissues and cells were analyzed by RT-qPCR using the $2^{-\Delta\Delta Cq}$ method for quantification (14). In detail, total RNA was extracted using the TRIzol™ Plus RNA Purification kit (cat. no. 12183555; Thermo Fisher Scientific, Inc.). Total RNA was reverse transcribed into cDNA using the All-in-One™ miRNA First-Strand cDNA Synthesis kit (cat. no. 18091050; Thermo Fisher Scientific, Inc.) according to the manufacturer's protocol. miR-1226-3p expression was evaluated using the SuperScript™ III Platinum™ SYBR™ One-Step Green qPCR kit (cat. no. 11736051; Thermo Fisher Scientific, Inc.). TNF receptor-associated factor 3 (TRAF3) mRNA expression was assayed using TaqMan™ Fast Advanced Master Mix (cat. no. 4444557; Thermo Fisher Scientific, Inc.). The sequences of the involved primers were as follows: miR-1226-3p-forward, 5'-GTCACCAGCCCTGTGT-3' and reverse, 5'-GCAGGGTCCGAGGTAATTC-3'; U6 forward, 5'-CTCGCTTCGGCAGCACA-3' and reverse, 5'-AACGCTTCACGAATTTGCGT-3'; TRAF3 forward, 5'-CTCACAAGTGCAGCGTCCAG-3' and reverse, 5'-GCTCCACTCCTTCAGCAGGTT-3'; and GAPDH forward, 5'-GTCTCCTCTGACTTCAACAGCG-3' and reverse, 5'-ACCACCCTGTTGCTGTAGCCAA-3'. The primers were designed and synthesized by Sangon Biotech Co., Ltd. miR-1226-3p expression was normalized to U6, which was used as the internal reference (15). The qPCR conditions for miRNA detection were as follows: 95˚C for 10 min, followed by 38 cycles at 95˚C for 1 min and 60˚C for 30 sec. The qPCR conditions for TRAF3 detection were as follows: 95˚C for 10 sec, followed by 40 cycles at 95˚C for 5 sec and 60˚C for 20 sec. GAPDH was used as the internal reference for mRNA.

Mutation site and target gene prediction. The potential targets of miR-1226-3p were predicted using TargetScan software (http://www.targetscan.org/vert_72/; version 7.2) (16-20). TargetScan predicts the biological targets of miRNAs by searching for the presence of conserved 8mer, 7mer and 6mer sites that match the seed region of each miRNA. The mutation in the 3'-untranslated region (3'-UTR) of TRAF3 was generated using the GeneArt™ Site-Directed Mutagenesis System according to the manufacturer's protocol (cat. no. A13282; Thermo Fisher Scientific, Inc.).

Apoptosis analysis. The apoptosis rate was analyzed using the Dead Cell Apoptosis kit with Annexin V-FITC and PI (cat. no. V13242; Thermo Fisher Scientific, Inc.). In detail, the cells were harvested and washed once in cold PBS ($1x10^6$ cells/tube). After centrifuging the washed cells in PBS

(300 x g at 4˚C for 5 min), the supernatant was discarded, the cells were resuspended in 1X Annexin-binding buffer (100 μl), and then Annexin V-FTIC (5 μl) and PI (1 μl) were added. After the mixture was incubated at room temperature for 15 min, the apoptosis rate was analyzed using a BD FACSVerse™ flow cytometer (BD Biosciences) with a 488-nm excitation laser. The data were analyzed using BD FACSuite™ version 1.01 (BD Biosciences). Cells in the right quadrants (early and late apoptosis) were chosen for apoptosis assay for quantification.

MTT assay. The proliferation of SaOS-2 cells was analysed using the MTT assay. SaOS-2 cells were seeded into 96-well plates at a density of $5x10^5$ cells/well. MTT reagent was added into the culture medium at a final concentration of 0.1 mg/ml. The purple formazan crystals were dissolved using 100 μl DMSO, and optical density was measured using a microplate reader (Multiskan Sky; Thermo Fisher Scientific, Inc.) at a wavelength of 570 nm (21).

Western blot analysis. The SaOS-2 cells were detached and then lysed with radioimmunoprecipitation assay (RIPA) buffer (cat. no. 89900; Thermo Fisher Scientific, Inc.) containing protease inhibitor (cat. no. 78420; Thermo Fisher Scientific, Inc.). Cold RIPA buffer (1 ml) was used for $5x10^6$ cells. The mixture was agitated for 30 min at 4˚C and then centrifuged at 300 x g at 4˚C for 5 min. The protein concentration of the aspirated supernatant was analyzed using the BCA Protein Assay kit (cat. no. ab102536; Abcam). Protein samples (30 μg/lane) were loaded and run at 80 V for 2 h via 12% SDS-PAGE. The proteins were transferred onto polyvinylidene fluoride membranes that were then immersed in 5% skimmed milk for 1 h for blocking at room temperature. The membranes were cut and incubated overnight at 4˚C separately with primary antibodies against TRAF3 (1:1,000; cat. no. ab36988; Abcam) and GAPDH (1:1,000; cat. no. ab181602; Abcam). After washing 3 times for 10 min each time at room temperature in TBS with 0.1% Tween-20, the membranes were incubated with HRP-conjugated goat anti-rabbit secondary antibody (1:500; cat. no. ab205718; Abcam) at room temperature for 2 h. The protein bands were visualized using Pierce™ ECL Western blotting substrate (cat. no. 32209; Thermo Fisher Scientific, Inc.). The images were acquired using the FluorChem System (ProteinSimple), and the software used for analysis was AlphaView Stand Alone (ProteinSimple; version 3.5.0).

Luciferase reporter assay. The luciferase reporter assay was performed using the Dual-Luciferase Reporter Assay System (cat. no. E1910; Promega Corporation). The 3'-UTR of the TRAF3 gene was amplified by PCR and cloned downstream of the luciferase gene in the pGL/Promoter vector (Sangon Biotech Co., Ltd.) to the wild-type plasmids. The *Renilla* luciferase gene in the vector acted as a control reporter for normalization. SaOS-2 cells were co-transfected with miR-1226-3p mimics and the luciferase-containing wild-type or mutant 3'-UTRs of TRAF3 using Lipofectamine® 2000 (cat. no. 11668019; Thermo Fisher Scientific, Inc.). The cells were collected after 24 h of transfection, and luciferase activity was analyzed according to the manufacturer's protocol.

Statistical analysis. Experiments were repeated 3 times independently. Statistical analysis was performed using GraphPad Prism version 5.0 (GraphPad Software, Inc.). All results were expressed as the mean ± SD. Overall survival was defined as the length of time from the date of cancer diagnosis to the date of death from any cause. The Kaplan-Meier method

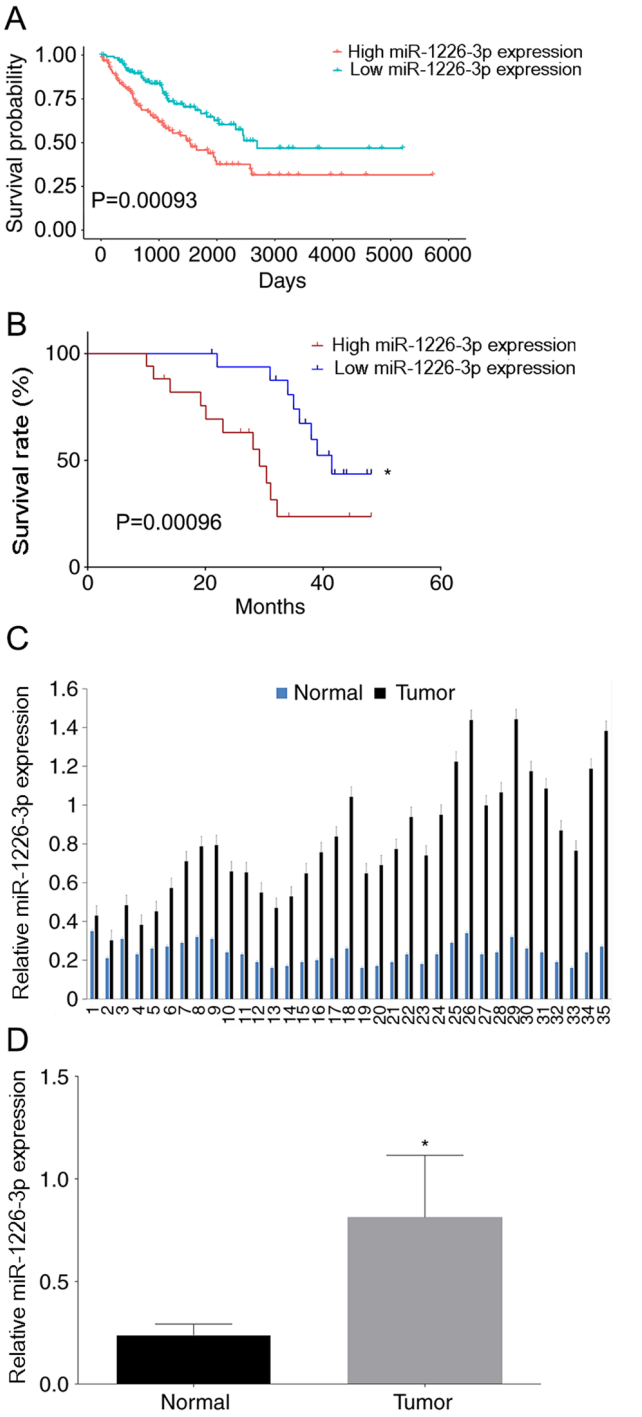

Figure 1. High miR-1226-3p expression decreases the survival rates of patients with osteosarcoma. (A) Survival analysis of 256 patients with sarcoma from TCGA database. The patients with sarcoma were divided into 2 groups according to the median miR-1226-3p expression value. (B) Survival analysis of 35 patients with osteosarcoma from West China Hospital. The patients with osteosarcoma were divided into 2 groups according to the median miR-1226-3p expression value. (C) miR-1226-3p expression in the 35 pairs of osteosarcoma and corresponding adjacent normal tissues was analyzed by reverse transcription-quantitative PCR. (D) Paired t-test of the mean miR-1226-3p expression values in tumor and normal tissues. Data are presented as the mean ± SD. Each experiment was repeated ≥3 times. *P<0.05. miR, microRNA.

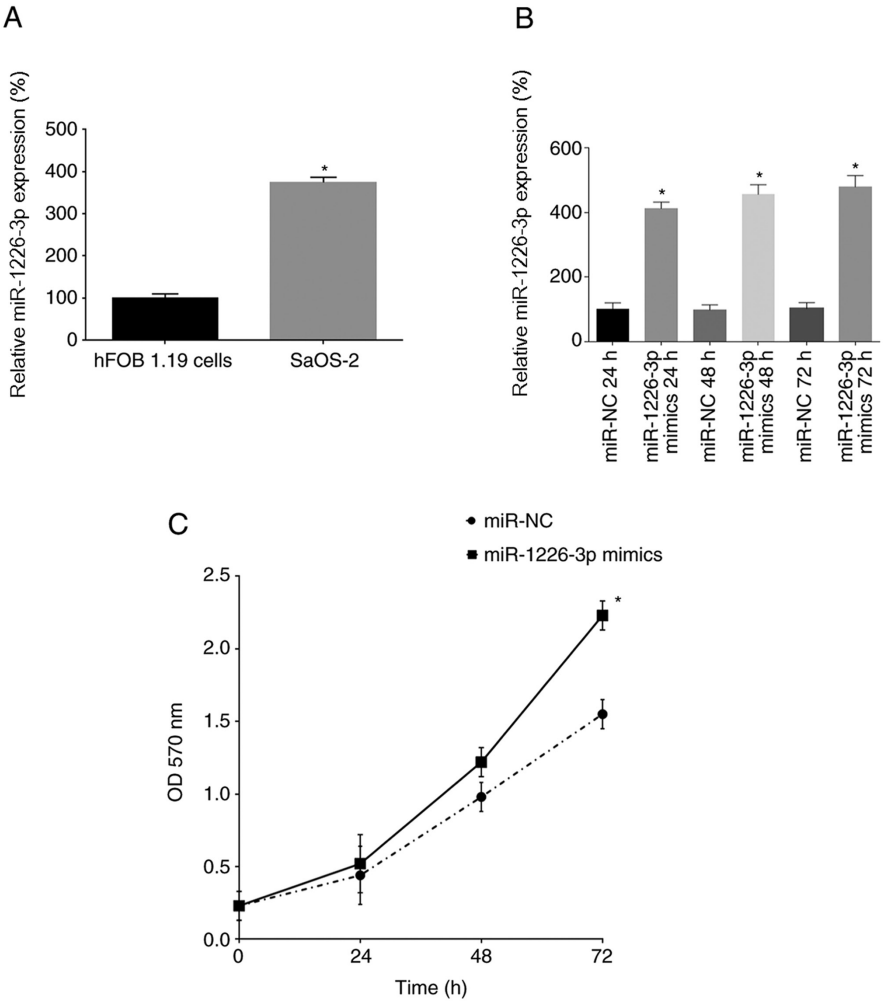

Figure 2. miR-1226-3p promotes SaOS-2 cell proliferation. (A) miR-1226-3p expression in hFOB 1.19 and SaOS-2 cells was analyzed by RT-qPCR. miR-1226-3p expression in hFOB 1.19 cells was arbitrarily defined as 100%. (B) miR-1226-3p mimics were transfected into SaOS-2 cells. After 24, 48 and 72 h, miR-1226-3p expression was analyzed by RT-qPCR. miR-1226-3p expression in the miR-NC-transfected cells was arbitrarily defined as 100%. (C) Cell proliferation was analyzed using the MTT assay at 0, 24, 48 and 72 h after miR-1226-3p mimic transfection. Data are presented as the mean ± SD. Each experiment was repeated ≥3 times. *P<0.05 vs. hFOB 1.19 or respective NC groups. miR, microRNA; RT-qPCR, reverse transcription-quantitative PCR; NC, negative control; OD, optical density.

was used to draw the survival curves, and the log-rank test was used to calculate the P-value. Differences between two groups were analyzed by Student's t-tests. The differences between pairs of tumor and normal tissues were analyzed by paired Student's t-test. The difference between two groups, such as miR-1226-3p expression in two different cell lines or in transfected or control cells, or the OD values in treated or control cells were assessed by unpaired Student's t-test. Differences among 3 groups were assessed by one-way ANOVA followed by Student-Newman-Keuls post hoc test. P<0.05 was considered to indicate a statistically significant difference.

Results

High miR-1226-3p expression is associated with lower overall survival rates. The role of miR-1226-3p was initially assessed in the survival of patients with sarcoma in TCGA database since osteosarcoma accounts for a major portion of sarcoma. There were 256 patients with sarcoma in the data frame. The median miR-1226-3p expression value was 0.97±1.03, and patients were divided into 2 groups based on the median miR-1226-3p expression value to perform survival analysis. It was revealed that patients with higher miR-1226-3p expression in tumor tissues had lower overall survival rates than patients with lower miR-1226-3p expression (Fig. 1A). Subsequently, survival was analyzed in the 35 matched pairs of osteosarcoma and adjacent normal tissues collected for the present study. miR-1226-3p expression in tissues was analyzed by RT-qPCR. The 35 patients with osteosarcoma patients were divided into 2 groups according to the median miR-1226-3p expression value (0.76), and then survival analysis was performed. The Kaplan-Meier method was used to draw the survival curves, and the log-rank test was used to calculate the P-value. Consistently with TCGA data, patients with higher miR-1226-3p expression in tumor tissues exhibited lower overall survival rates than patients with lower miR-1226-3p expression (Fig. 1B). Moreover, miR-1226-3p expression in tumor tissues was higher than that in adjacent normal tissues (Fig. 1C), with the mean miR-1226-3p expression value in tumor tissues being significantly higher than that in normal tissues (Fig. 1D). Thus, it was hypothesized that miR-1226-3p served a role in the molecular mechanism of osteosarcoma.

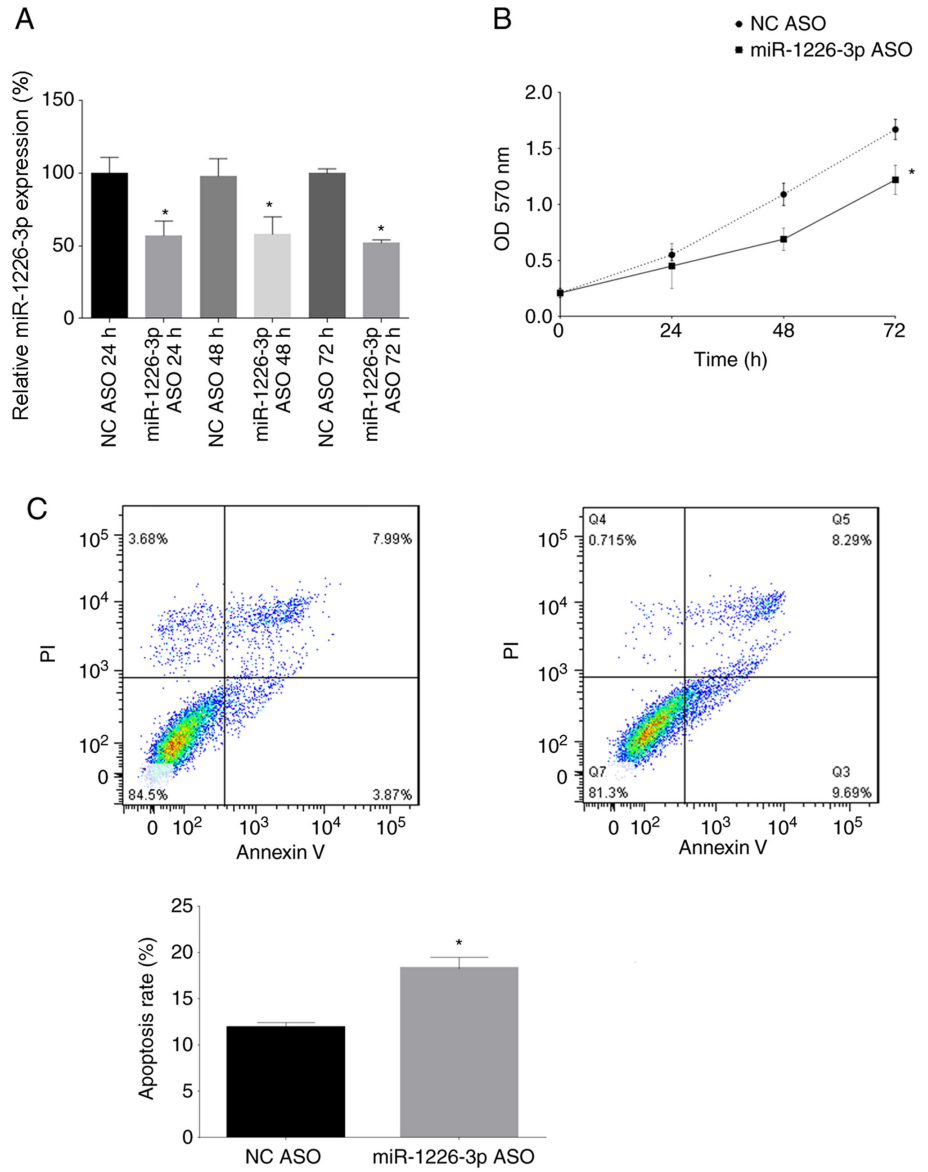

Figure 3. Inhibition of miR-1226-3p decreases SaOS-2 cell proliferation and promotes apoptosis. (A) miR-1226-3p ASOs were transfected into SaOS-2 cells. After 24, 48 and 72 h of transfection, miR-1226-3p expression was analyzed by reverse transcription-quantitative PCR. miR-1226-3p expression in the NC-ASO-transfected cells was arbitrarily defined as 100%. (B) Cell proliferation was analyzed using the MTT assay at 0, 24, 48 and 72 h after miR-1226-3p-ASO transfection. (C) Apoptosis rate was analyzed by annexin V/PI double staining 24 h after miR-1226-3p-ASO transfection. Data are presented as the mean ± SD. Each experiment was repeated ≥3 times. *P<0.05 vs. respective NC groups. miR, microRNA; NC, negative control; ASO, antisense oligonucleotide; OD, optical density.

miR-1226-3p promotes SaOS-2 cell proliferation. Cell experiments were used to analyze the function of miR-1226-3p in osteosarcoma. First, miR-1226-3p expression was analyzed in hFOB 1.19 and SaOS-2 cells by RT-qPCR. It was revealed that SaOS-2 cells exhibited significantly higher miR-1226-3p expression than hFOB 1.19 cells (Fig. 2A). Next, miR-1226-3p was overexpressed in SaOS-2 cells by transfection with miR-1226-3p mimics, and miR-1226-3p expression was analyzed at 24, 48 and 72 h after transfection. miR-1226-3p mimics significantly increased miR-1226-3p expression in SaOS-2 cells transfected for 24, 48 and 72 h compared with their respective NCs (Fig. 2B). Using MTT analysis, the proliferation of SaOS-2 cells was assessed after transfection with the miR-1226-3p mimics, revealing that miR-1226-3p mimics significantly promoted the proliferation of SaOS-2 cells after 72 h (Fig. 2C).

Inhibition of miR-1226-3p decreases SaOS-2 cell proliferation and promotes apoptosis. miR-1226-3p expression was inhibited in SaOS-2 cells by transfection with miR-1226-3p ASOs. At 24, 48 and 72 h after transfection, miR-1226-3p expression in SaOS-2 cells was assessed by RT-qPCR. miR-1226-3p ASOs significantly decreased miR-1226-3p expression in SaOS-2 cells transfected for 24, 48 and 72 h compared with their respective NCs (Fig. 3A). In addition, the proliferation of SaOS-2 cells was analyzed 24, 48 and 72 h after transfection with miR-1226-3p ASOs, revealing that the miR-1226-3p ASOs significantly inhibited the proliferation of SaOS-2 cells after 72 h (Fig. 3B). Finally, the apoptosis rate of SaOS-2 cells was assessed 24 h after transfection with the miR-1226-3p ASOs, revealing that the miR-1226-3p ASOs significantly promoted the apoptosis rate of SaOS-2 cells (Fig. 3C).

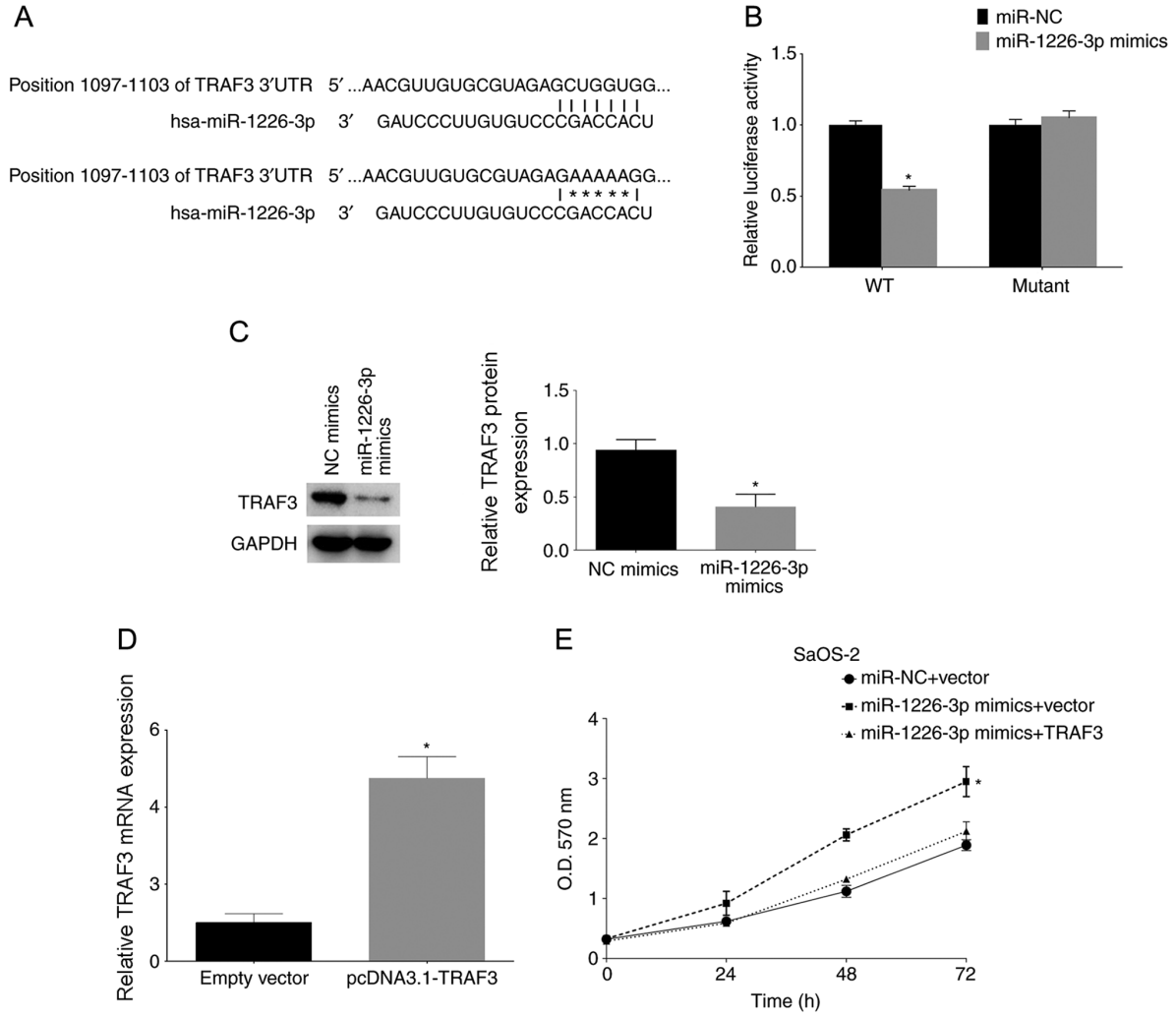

Figure 4. TRAF3 is targeted by miR-1226-3p. (A) miR-1226-3p potential binding sites and mutation sites (positions 20-26) in the 3'-UTR of the TRAF3 gene. (B) SaOS-2 cells were co-transfected with miR-1226-3p mimics or miR-NC and luciferase reporter vectors containing WT or mutant 3'-UTRs. (C) TRAF3 protein expression following transfection with miR-1226-3p mimics or miR-NC was analyzed by western blotting. GAPDH was used as the internal control. (D) SaOS-2 cells were transfected with TRAF3 overexpression plasmid (pcDNA3.1-TRAF3), and TRAF3 mRNA expression was assayed by reverse transcription-quantitative PCR. (E) Proliferation analysis of SaOS-2 cells transfected with miR-1226-3p mimics and TRAF3 overexpression plasmid was performed via MTT assay at 24, 48 and 72 h after transfection. Data are presented as the mean ± SD. Each experiment was repeated ≥3 times. *P<0.05. miR, microRNA; NC, negative control; UTR, untranslated region; WT, wild-type; OD, optical density; TRAF3, TNF receptor-associated factor 3.

miR-1226-3p targets TRAF3. The possible genes targeted by miR-1226-3p were analyzed using bioinformatics methods. It was revealed that the TRAF3 gene was targeted by miR-1226-3p. The binding sites are shown in Fig. 4A. TRAF3 wild-type and mutant 3'-UTRs were cloned and inserted into luciferase reporter plasmids. The luciferase assay results revealed that miR-1226-3p mimics significantly decreased luciferase activity by directly binding to the 3'-UTR of TRAF3; however, mutation of the putative miR-1226-3p binding sites in the 3'-UTR of TRAF3 abrogated the luciferase response to miR-1226-3p mimics (Fig. 4B). Subsequently, TRAF3 protein expression was analyzed after miR-1226-3p mimic transfection, revealing that miR-1226-3p mimic transfection significantly decreased TRAF3 protein expression in SaOS-2 cells, as shown by western blotting (Fig. 4C). Finally, SaOS-2 cells were transfected with miR-1226-3p mimics and TRAF3 overexpression plasmid (pcDNA3.1-TRAF3). The effect of pcDNA3.1-TRAF3 was confirmed by RT-qPCR (Fig. 4D). The results of the MTT assay of the TRAF3-overexpressing cells after miR-1226-3p mimic transfection revealed that TRAF3 overexpression reversed the proliferative effect of miR-362-3p mimics on these cells (Fig. 4E).

Discussion

The present study analyzed the function of miR-1226-3p in osteosarcoma. It was revealed that higher miR-1226-3p expression decreased the overall survival rates of patients with osteosarcoma, and data from experiments in SaOS-2 cells demonstrated that miR-1226-3p promoted cell proliferation. Moreover, miR-1226-3p inhibition increased the apoptosis rate in osteosarcoma cells. Furthermore, TRAF3 was identified as a target gene of miR-1226-3p. To the best of our knowledge, the current study is the first to reveal the role of miR-1226-3p in osteosarcoma.

According to the apoptosis analysis, there appeared to be some late apoptotic cells in both groups, for which there may be two possible reasons: One is that the duration of PI staining,

since as the duration of PI staining increases, the number of PI^+ cells may increase, and the other is that there may be some dead cells following transfection and PBS washing.

A similar study has revealed that hepatocellular carcinoma tissues exhibit higher miR-1226-3p expression compared with normal tissues (11). Consistently, the current data indicated that osteosarcoma tissues exhibited higher miR-1226-3p expression than normal tissues. In addition to the aforementioned study, the present study revealed that miR-1226-3 targeted the TRAF3 protein to serve its role in osteosarcoma. However, another study involving human breast cancer cell lines has demonstrated that miR-1226 targets mucin 1 oncoprotein and induces cell death (9). Therefore, it seems that miR-1226-3 may serve different roles in different types of cancer.

The TRAF3 protein has an important role in the immune response. TRAF proteins are basic components of signaling pathways activated by TNF receptor or toll-like receptor family members (22). TRAF3, which is a specific TRAF protein, is involved in positive and negative regulatory functions in multiple signaling pathways (10). TRAF3 is a highly versatile regulator that positively controls type I interferon production but negatively regulates mitogen-activated protein kinase activation and alternative nuclear factor-κB signaling (23,24). Notably, miR-214 functions as an oncogene in human osteosarcoma by targeting TRAF3 (25). Thus, TRAF3 was further analyzed in the present study.

The role of TRAF3 in cancer has been the subject of several studies. The TRAF3 protein acts as an anti-inflammatory factor and is required for optimal innate immunity in myeloid cells (26). Furthermore, the TRAF3 gene is a novel tumor suppressor gene in macrophages (26). In addition, the TRAF3 protein regulates the oncogenic proteins Pim2 and c-Myc to reduce survival in normal and malignant B cells (27). Moreover, the TRAF3 protein can interact with the glucocorticoid modulatory element-binding protein 1 protein and modulate its anti-apoptotic function (28). The current data indicated that TRAF3 overexpression partly decreased the proliferative effect of miR-1226-3p in SaOS-2 cells. TRAF3 overexpression may therefore also increase apoptosis, which will be investigated in a future study.

The present study has some limitations. First, SaOS-2 cells were used as models and hFOB 1.19 cells were used as controls. hFOB 1.19 cells are derived from osteoblasts, while Saos-2 cells are human osteosarcoma cells with several osteoblastic features, and they lack both Rb and intact p53 (29,30). However, the p53 protein is mutated in most patients with osteosarcoma (80-90%) (31). Therefore, p53 may affect the function of miR-1226-3p in osteosarcoma, which will be investigated in a future study. Another limitation is that there is a lack of comparison in miR-1226 expression across a panel of OS cell lines, as well as a lack if *in vivo* data.

The present results revealed that TRAF3 may be inhibited by miR-1226-3p, suggesting that miR-1226-3p may serve a role in the immune response network. This study has clinical significance since it revealed a possible molecular target and indicator of osteosarcoma prognosis. Patients with osteosarcoma may benefit from miR-1226-3p regulation, which requires further investigation. Overall, the present study revealed that miR-1226-3p may serve a tumor-promoting role in osteosarcoma.

Acknowledgements

Not applicable.

Funding

The present study was supported by the Innovation and Cultivation Foundation of Naval General Hospital (grant no. CXPY-201818).

Availability of data and materials

All data generated or analyzed during this study are included in this published article. The datasets generated and/or analyzed during the current study are available in the Xena Browser (https://xenabrowser.net/).

Authors' contributions

YL, TA and JL collected patient data. YL, DS and TA performed PCR, western blotting and other molecular experiments. QY performed the bioinformatics analysis and luciferase reporter assay. YL and SN contributed to the study design and manuscript writing. JL and SN contributed to data analysis and revising the manuscript for important intellectual content. All authors confirm the authenticity of the raw data, and have read and approved the final manuscript.

Ethics approval and consent to participate

The Ethics Committee of Sichuan University (Chengdu, China) approved the usage of the patients' clinical data and tissue samples, and all patients or their guardians provided written informed consent for the use of their clinical information and tissue samples.

Patient consent for publication

Not applicable.

Competing interests

The authors declare that they have no competing interests.

References

1. Mirabello L, Troisi RJ and Savage SA: Osteosarcoma incidence and survival rates from 1973 to 2004: Data from the surveillance, epidemiology, and end results program. Cancer 115: 1531-1543, 2009.
2. Biermann JS, Adkins DR, Agulnik M, Benjamin RS, Brigman B, Butrynski JE, Cheong D, Chow W, Curry WT, Frassica DA, *et al*: Bone cancer. J Natl Compr Canc Netw 11: 688-723, 2013.
3. Mirabello L, Troisi RJ and Savage SA: International osteosarcoma incidence patterns in children and adolescents, middle ages and elderly persons. Int J Cancer 125: 229-234, 2009.
4. Xia L, Zheng R, Xu Y, Xu X, Zhang S, Zeng H, Lin L and Chen W: Incidence and mortality of primary bone cancers in China, 2014. Chin J Cancer Res 31: 135-143, 2019.
5. Carthew RW and Sontheimer EJ: Origins and mechanisms of miRNAs and siRNAs. Cell 136: 642-655, 2009.
6. Sasaki R, Osaki M and Okada F: MicroRNA-based diagnosis and treatment of metastatic human osteosarcoma. Cancers (Basel) 11: 553, 2019.

7. Sampson VB, Yoo S, Kumar A, Vetter NS and Kolb EA: MicroRNAs and potential targets in osteosarcoma: Review. Front Pediatr 3: 69, 2015.
8. Tomczak K, Czerwińska P and Wiznerowicz M: The cancer genome atlas (TCGA): An immeasurable source of knowledge. Contemp Oncol (Pozn) 19: A68-A77, 2015.
9. Jin C, Rajabi H and Kufe D: miR-1226 targets expression of the mucin 1 oncoprotein and induces cell death. Int J Oncol 37: 61-69, 2010.
10. Zhou Q, Zeng H, Ye P, Shi Y, Guo J and Long X: Differential microRNA profiles between fulvestrant-resistant and tamoxifen-resistant human breast cancer cells. Anticancer Drugs 29: 539-548, 2018.
11. Chen X, Tan W, Li W, Li W, Zhu S, Zhong J, Shang C and Chen Y: miR-1226-3p promotes sorafenib sensitivity of hepatocellular carcinoma via downregulation of DUSP4 expression. J Cancer 10: 2745-2753, 2019.
12. Amin MB, Edge SB, Greene FL, Byrd DR, Brookland RK, Washington MK, Gershenwald JE, Compton CC, Hess KR, Sullivan DC, *et al* (eds): AJCC Cancer Staging Manual. 8th edition. Springer, Heidelberg, 2017.
13. Wickham H, François R, Henry L and Müller K: dplyr: A grammar of data manipulation. R package version 0.7.6, 2018. https://CRAN.R-project.org/package=dplyr. Accessed December 16, 2019.
14. Livak KJ and Schmittgen TD: Analysis of relative gene expression data using real-time quantitative PCR and the 2(-Delta Delta C(T)) method. Methods 25: 402-408, 2001.
15. Song B, Zhang C, Li G, Jin G and Liu C: miR-940 inhibited pancreatic ductal adenocarcinoma growth by targeting MyD88. Cell Physiol Biochem 35: 1167-1177, 2015.
16. Lewis BP, Burge CB and Bartel DP: Conserved seed pairing, often flanked by adenosines, indicates that thousands of human genes are microRNA targets. Cell 120: 15-20, 2005.
17. Friedman RC, Farh KK, Burge CB and Bartel DP: Most mammalian mRNAs are conserved targets of microRNAs. Genome Res 19: 92-105, 2009.
18. Grimson A, Farh KK, Johnston WK, Garrett-Engele P, Lim LP and Bartel DP: MicroRNA targeting specificity in mammals: Determinants beyond seed pairing. Mol Cell 27: 91-105, 2007.
19. Garcia DM, Baek D, Shin C, Bell GW, Grimson A and Bartel DP: Weak seed-pairing stability and high target-site abundance decrease the proficiency of lsy-6 and other microRNAs. Nat Struct Mol Biol 18: 1139-1146, 2011.
20. Lee S, Paulson KG, Murchison EP, Afanasiev OK, Alkan C, Leonard JH, Byrd DR, Hannon GJ and Nghiem P: Identification and validation of a novel mature microRNA encoded by the merkel cell polyomavirus in human merkel cell carcinomas. J Clin Virol 52: 272-275, 2011.
21. Zhao H, Zheng Y, You J, Xiong J, Ying S, Xie L, Song X, Yao Y, Jin Z and Zhang C: Tumor suppressor role of miR-876-5p in gastric cancer. Oncol Lett 20: 1281-1287, 2020.
22. Hacker H, Tseng PH and Karin M: Expanding TRAF function: TRAF3 as a tri-faced immune regulator. Nat Rev Immunol 11: 457-468, 2011.
23. Tseng PH, Matsuzawa A, Zhang W, Mino T, Vignali DA and Karin M: Different modes of ubiquitination of the adaptor TRAF3 selectively activate the expression of type I interferons and proinflammatory cytokines. Nat Immunol 11: 70-75, 2010.
24. Perkins DJ, Polumuri SK, Pennini ME, Lai W, Xie P and Vogel SN: Reprogramming of murine macrophages through TLR2 confers viral resistance via TRAF3-mediated, enhanced interferon production. PLoS Pathog 9: e1003479, 2013.
25. Rehei AL, Zhang L, Fu YX, Mu WB, Yang DS, Liu Y, Zhou SJ and Younusi A: MicroRNA-214 functions as an oncogene in human osteosarcoma by targeting TRAF3. Eur Rev Med Pharmacol Sci 22: 5156-5164, 2018.
26. Lalani AI, Luo C, Han Y and Xie P: TRAF3: A novel tumor suppressor gene in macrophages. Macrophage (Houst) 2: e1009, 2015.
27. Whillock AL, Mambetsariev N, Lin WW, Stunz LL and Bishop GA: TRAF3 regulates the oncogenic proteins Pim2 and c-Myc to restrain survival in normal and malignant B cells. Sci Rep 9: 12884, 2019.
28. Kotsaris G, Kerselidou D, Koutsoubaris D, Constantinou E, Malamas G, Garyfallos DA and Hatzivassiliou EG: TRAF3 can interact with GMEB1 and modulate its anti-apoptotic function. J Biol Res (Thessalon) 27: 7, 2020.
29. Marcellus RC, Teodoro JG, Charbonneau R, Shore GC and Branton PE: Expression of p53 in Saos-2 osteosarcoma cells induces apoptosis which can be inhibited by Bcl-2 or the adenovirus E1B-55 kDa protein. Cell Growth Differ 7: 1643-1650, 1996.
30. Li W, Fan J, Hochhauser D, Banerjee D, Zielinski Z, Almasan A, Yin Y, Kelly R, Wahl GM and Bertino JR: Lack of functional retinoblastoma protein mediates increased resistance to antimetabolites in human sarcoma cell lines. Proc Natl Acad Sci USA 92: 10436-10440, 1995.
31. Kansara M, Teng MW, Smyth MJ and Thomas DM: Translational biology of osteosarcoma. Nat Rev Cancer 14: 722-735, 2014.